J Appl Electrochem (2007) 37:1237–1243
DOI 10.1007/s10800-007-9377-2

ORIGINAL PAPER

# Investigation of optimal conditions for zinc electrowinning from aqueous sulfuric acid electrolytes

**P. Guillaume · N. Leclerc · C. Boulanger · J. M. Lecuire · François Lapicque**

Received: 17 January 2007 / Revised: 13 July 2007 / Accepted: 13 July 2007 / Published online: 3 August 2007


**Abstract** Results are reported of an experimental investigation of the effects of aqueous zinc(II) and sulfuric acid concentrations on current efficiencies and deposit morphologies of metallic zinc, aimed at designing a process for zinc recovery from solid industrial wastes by leaching and electrodeposition. Voltammetry and chronopotentiometry of additive-free solutions of zinc(II) sulfate and sulfuric acid were used to determine the zinc(II) reduction kinetics, prior to investigating the deposition in a Hull cell to observe the effects of the current density and the bath composition on current efficiencies and deposit morphologies. For a current density of 45 mA $cm^{-2}$, best performance was obtained with zinc(II) concentrations of the same order of magnitude as the $H^+$ concentration; too acidic solutions resulted in lower current yields and pronounced 3-D growth of the deposit.

**Keywords** Zinc deposition · Sulfuric solutions · Hull cell · Current efficiency · Zinc morphology

## 1 Introduction

More than 80% of the world's primary zinc is produced by so-called roast-leach-electrowin processes e.g., [1–3], fed with sulfide mineral concentrates that are oxidised to oxides during high temperature roasting in air. The metal oxide product is then leached with aqueous sulfuric acid; such processes could also be used for zinc recovery from residues of metallurgical processes. In particular, jarosite or haematite residues can contain significant amounts of zinc, and conventional lead blast furnaces are the source of significant emission of zinc oxide fumes, yielding fine oxide dusts after cooling of the exhaust gases. Leaching results in the formation of zinc(II) sulfate in the aqueous sulfuric acid and the metal is then produced by electrodeposition at ambient/moderate temperatures with current densities of the order of 50 mA $cm^{-2}$.

The effect of electrolyte composition on both the current yield and the deposit morphology has been investigated extensively [4–9], but the conclusions reported are not perfectly consistent: according to Adcock et al. [6], higher current yields are obtained for high $H^+/Zn^{II}$ ratios, in contradiction with other papers [7–10]. In particular Saba and Elsherief [8] reported high yields for zinc(II) concentrations above 0.6 M and moderate concentrations of acid. Zinc deposition is linked to hydrogen evolution, which may appear as both a side and necessary electrode process in the formation of the metal [11].

The presence of impurities may affect the deposition mechanism, as described below: the presence of alkali and alkaline earth metals was shown to be detrimental to zinc deposition by Turomshina and Stender [12] and by Ault et al. [13]. Heavy metals were reported to change the mechanism of the deposition, as with lead [14], manganese [10], or antimony [15, 16]; any species that could catalyse hydrogen evolution have detrimental effects on current efficiencies for zinc deposition, such that they have to be depleted from the electrolyte to extremely low concentrations. In addition, organic substances e.g., glue [8, 15, 17], urea or naphtol derivatives [6] have been commonly employed. Also, Muresan et al. [18] investigated the effect

P. Guillaume · N. Leclerc · C. Boulanger · J. M. Lecuire · F. Lapicque
Laboratoire d'Electrochimie des Matériaux, UMR CNRS 7555, Université P. Verlaine, CP 87811, Metz 57078, France

F. Lapicque (✉)
Laboratoire des Sciences du Génie Chimique, CNRS-ENSIC, BP 20451, Nancy 54001, France
e-mail: Francois.lapicque@ensic.inpl-nancy.fr

of additives for the case of electrolyte solutions obtained by leaching of industrial wastes. As for other metals, the presence of additives is known to inhibit the deposition rate, resulting in smaller grains of different orientations: as mentioned in [6] fine-grained, compact zinc consists of crystals either with random or (101) orientations, whereas (110), (100), (211) and (112) orientations predominate in coarse-grained deposits. In addition, a strong correlation between the current efficiency and the morphology of zinc deposits was shown by these authors.

The project for which results are reported below, is part of a research programme for the design and operation of a process for zinc recovery from zinc(II)-containing industrial wastes, combining electrochemical leaching and electrodeposition [19]: the relative rates of the two steps of the process govern the composition of the electrolyte solution, and the operating parameters have to be searched for the optimal conditions of zinc deposition in terms of current efficiency and morphology of the zinc produced. Therefore, this investigation aimed to define suitable ranges of zinc(II) and sulfuric acid concentrations in the electrolyte solutions, using pure zinc sulfate-sulfuric acid only. Since the combined process is to be operated with only sluggish circulation of the fluid in the various parts of the cell, the effect of hydrodynamics on the deposition was not investigated. Voltammetry and chronopotentiometry were used for preliminary tests, prior to investigating the deposition in a Hull cell, as used previously [10, 16] with other deposition baths, allowing a large range of current density to be investigated. The effects of the bath composition on current efficiencies and deposit morphologies were also determined.

## 2 Experimental section

### 2.1 Chemicals

Solutions were prepared with analytical grade zinc sulfate heptahydrate (Riedel de Haën), 18 M sulfuric acid (Analytical grade, Acros Chemicals), and deionised water. Zinc(II) concentrations in the prepared solutions, as well as in samples, were determined by atomic absorption using an AA 240 FS (Varian) spectrophotometer. No additives were employed to emulate a process for zinc recovery by coupled leaching and deposition from ores or oxide wastes. The various solutions were not de-oxygenated, so that experimental conditions were closer to those in industrial winning processes.

### 2.2 Experimental devices

Electrochemical measurements were carried out using a glass cell with three electrodes. The working electrode was a rotating stainless steel disc, 6 mm in diameter. Rotation of the electrode was controlled by a CVT 101 T, (Tacussel). A stationary platinum disc with a diameter of 10 mm (Radiometer) was the counter electrode. Potentials were referred to the saturated calomel electrode, SCE (Radiometer) provided with a saline bridge filled with 1 M $KNO_3$.

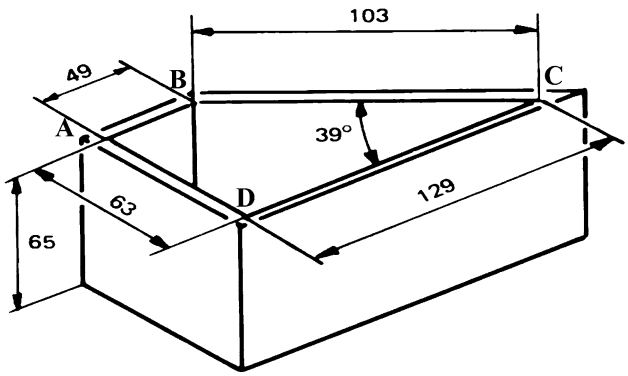


**Fig. 1** Schematic view of the Hull cell. Dimensions in mm

The Hull cell employed (Kocour Company Inc.) was a 65 mm deep trapezoidal pool with a volume of 267 $cm^3$. The dimensions of the cell obeyed the usual standards of Hull cells (Fig. 1). The lead anode was 63 mm long; the cathode (l = 103 mm) made a 39° angle with the longer insulated plate separating the two electrodes. The height of the liquid, H, in the cell was fixed at 49 mm for all tests. Although most experiments were carried out with a stainless steel plate cathode, additional tests were made with aluminium for comparison, since Al is used as the cathode material for industrial zinc electrowinning. The local electrode potential was measured using a home-made Luggin capillary, which could be moved along the electrode: the extremity of the syringe needle was at circa 1 mm from the cathode surface, at location *x* from the cell edge. The electrodes were connected to the ELC (AL 781NX) electrical current supply. The syringe-based Luggin capillary was connected to the SCE reference, allowing the value for the local electrode potential to be measured.

## 3 Electrochemical investigation of the deposition

### 3.1 Investigations at the disc electrode

Zinc deposition on the stainless steel disc electrode in 0.5 M $H_2SO_4$, 0.5 M $ZnSO_4$ solution at ambient temperature, changes the nature of the substrate and the surface state. Initially, chronopotentiometric measurements were carried out at 45 mA $cm^{-2}$ using a freshly polished stainless steel surface, without rotation of the disc. As shown in Fig. 2, the electrode potential decreased from an initial

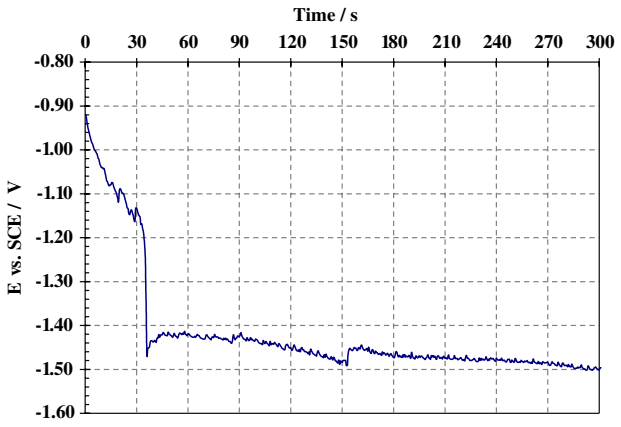


**Fig. 2** Chronopotentiogram for stationary stainless steel disc electrode at 45 mA $cm^{-2}$. Solution: 0.5 M $ZnSO_4$, 0.5 M $H_2SO_4$

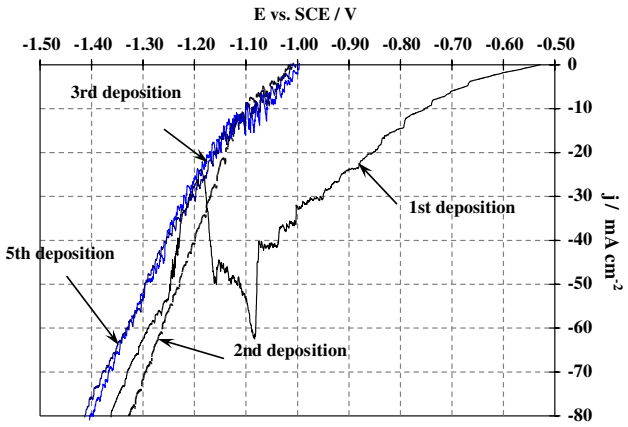


**Fig. 3** Voltammograms for zinc deposition from a 0.5 M $ZnSO_4$, 0.5 M $H_2SO_4$ solution on stainless steel RDE at 400 rpm

value of −0.92 V vs. SCE, corresponding to the formation a zinc layer on the cathode surface. After a sudden change at 35 s, the potential remained fairly constant near −1.45 V (SCE), and the electrode behaved more like a zinc surface. Optical and microscopic observation of the surface obtained confirmed the coverage of the electrode surface, in spite of the irregular appearance of the deposit.

Further chronopotentiometric experiments were made on freshly deposited surfaces with the disc rotating at 400 rpm: the current was fixed at a selected value, the potential was observed to attain a steady level within 10 s, then the current was increased and the measurement repeated. At the end of the series, the procedure was repeated, starting from the lowest current. The discrete *j–E* variation obtained was found to be reproducible within a few mV, provided that the disc surface was totally covered by the Zn deposit.

In addition, voltammograms of the rotating disc electrode were recorded by scanning from the open circuit potential to −1.40 V vs. SCE at 5 mV $s^{-1}$. Correction of the *j–E* data for uncompensated ohmic potential drop was made using the resistance determined by impedance spectroscopy from the high frequency intercept on the real impedance axis.

As shown in Fig. 3, in the first voltammogram of the polished stainless steel surface, on the negative-going potential scan from −0.5 V vs. SCE, the (net) reduction current increased in magnitude, due to hydrogen evolution on the stainless steel, until a current peak occurred at ca. −1.1 V vs. SCE, beyond which it decayed, until at <−1.2 V vs. SCE it again increased. After reaching the negative potential limit (−1.4 V vs. SCE) the RDE surface was observed to be covered with zinc, unsurprisingly as $E^0_{Zn^{2+}/Zn} = -1.008$ V vs. SCE. As the exchange current densities for hydrogen evolution 1 M $H_2SO_4$ are: $j_0(H_2,Cr) = 3.98 \times 10^{-3}$ A $m^{-2}$ and $j_0(H_2,Fe) = 1.58 \times 10^{-2}$ A $m^{-2}$, whereas $j_0(H_2,Zn) = 3.16 \times 10^{-7}$ A $m^{-2}$ [20] it is most likely that the current peak at ca. −1.1 V vs. SCE was due to hydrogen evolution on the stainless steel substrate being inhibited by deposition of zinc, with its much smaller hydrogen exchange current density.

Subsequent *j–E* data were recorded with the same zinc-plated electrode surface, without any further preparation, the open circuit potential then ranging from −1.00 to −1.05 V vs. SCE, in agreement with previous investigations [8]. The profile of the second voltammogram followed closely that of the first potential scan once the electrode surface had been covered by zinc. Subsequent *j–E* data for the same conditions exhibited perfect reproducibility, as Zn deposition occurred on the zinc surface of growing thickness.

### 3.2 j–E Curves in the Hull cell

Chronopotentiometric experiments were carried out in the Hull cell, with a constant current imposed to the stainless steel or Al substrate electrode. The potential difference between the plate electrode and the capillary usually attained a steady value within 10 s. Potential measurements were made at five locations along the plate, corresponding to five values of the current density (see following section). The potentials measured during the two first minutes of deposition differed significantly from those recorded after 5 min, because of the formation of a zinc deposit on most of the substrate electrode. Figure 4 gives an example of the variation obtained in the Hull cell; deposition occurred on Al at potentials nearly 70 mV more negative than on stainless steel, but with comparable potential dependence of the rate. These profiles were compared to the (*j–E*) variations measured with the stainless steel RDE, either by voltammetry or by steady-state measurements. These two

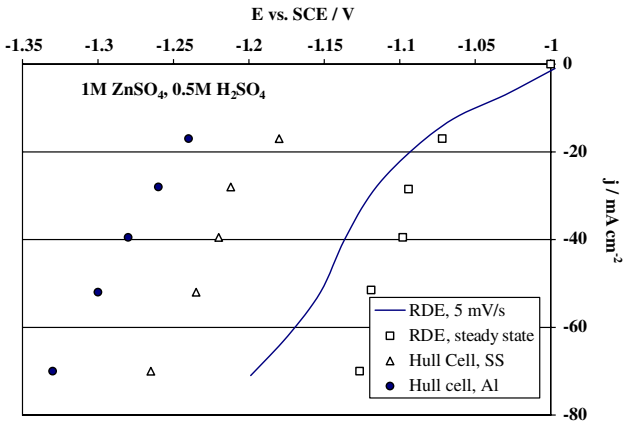


**Fig. 4** *j–E* variations measured in 1 M $ZnSO_4$, 0.5 M $H_2SO_4$ solution on the stainless steel RDE and in the Hull cell. Data obtained on the RDE (400 rpm) were corrected for uncompensated ohmic drop

series of data were corrected for ohmic potential losses. Basically, the profiles of steady-state measurements on the two electrode designs were found to be similar (Fig. 4), in spite of the 100 mV negative shift of potentials in the Hull cell, which might have been due to the different measurement techniques used. The data recorded by continuous scanning of the potential were consistent with, though with a lower potential dependence than the (*j–E*) variation measured at steady state with the same electrode.

## 4 Zinc deposition in the Hull cell

### 4.1 Current density and current efficiency in the Hull cell

The current density on the cathode surface of the Hull cell [21] decays with distance *x* from the side (B—Fig.1) closer to the anode. The primary distribution of current density in the cell obeys the empirical equation given by norm DIN 50950 [22]:

$$j(x) = \frac{I}{Hl}\left[2.33\log\left(\frac{1}{x}\right) - 0.08\right] \quad (1)$$

where *j* is in mA $cm^{-2}$, the global current *I* is in A, and dimensions *H*, *l*, and *x* are in cm. As e.g., Fig. 4 showed that zinc(II) reduction without additives occurs with very low overpotentials, the above equation for the primary current density distribution was assumed to hold for zinc deposition on the cathode; furthermore, the regions of the cathode close to edges B and C (Fig. 1), with extreme current density values were not considered in the analysis.

The overall current was fixed to 3.5 A, corresponding to an average current density of ca. 70 mA $cm^{-2}$. Deposition was carried out for 10 min and the electrode was removed from the cell, rinsed carefully with water and dried. Assuming that the deposition current efficiency was equal to 1, the theoretical average thickness of the deposit was calculated at 13 μm.

The overall deposition yield was deduced by weighing the zinc deposit formed at the cathode, $m_{Zn}$:

$$\Phi = \frac{m_{Zn}}{M_{Zn}} \cdot \frac{2F}{I\Delta t} \quad (2)$$

where $M_{Zn}$ is equal to 65.38 g $mol^{-1}$ and $\Delta t$ represents the duration of zinc deposition.

The influence of the current density on the current efficiency was investigated in three zones on the cathode surface, with the corresponding ranges of current density:

$$\begin{array}{lll} \text{Zone 1} & 1.50 < x < 2.50\text{cm} & 91.6 < j < 124.3\text{mA cm}^{-2} \\ \text{Zone 2} & 4.65 < x < 5.65\text{cm} & 3.94 < j < 51.8\text{mA cm}^{-2} \\ \text{Zone 3} & 6.20 < x < 6.70\text{cm} & 28.4 < j < 33.4\text{mA cm}^{-2} \end{array} \quad (3)$$

After optical and SEM observations of the deposit in the central part of each zone, protective adhesive tape was applied at the borders of the zone investigated, and the electrodeposited zinc on the plate was dissolved totally in 6 M HCl solution for subsequent analysis. The plate was rinsed and the liquid fractions collected. Analysis of the acidic solutions collected yielded the number of moles of zinc, $n_{12}$, deposited on the plate for $x_1 < x < x_2$. The current efficiency of Zn deposition in region ($x_1$, $x_2$) was calculated by:

$$\Phi_{12} = n_{12}\frac{2F}{\Delta t H \int_{x_1}^{x_2} j(x)dx} \quad (4)$$

The average current density, $j_{12}$, was deduced straightforwardly from the local current density given in Eq. (1):

$$j_{12} = \frac{1}{(x_2 - x_1)}\int_{x_1}^{x_2} j(x)dx \quad (5)$$

From the estimated precision in adjusting the insulating tape, the precision in the abscissae difference ($x_2 - x_1$) was estimated to be ca. one millimetre: for zone 2, the uncertainty in determination of the local current yield was estimated at ±10 %, whereas the overall efficiency Φ could be determined within 4%, as shown by replicate experiments. In spite of this level of uncertainty, values for $\Phi_{12}$ were compared to those for Φ.

For a few experiments, finer variations of the current efficiency versus current density were also determined by dividing the plate area into nine rectangular sections; the average current density and current efficiency in each section were calculated using Eqs. 5 and 4, respectively.

### 4.2 Influence of the current density on the deposit morphology

The morphology of the deposit was not influenced markedly by the nature of the cathode material; zinc morphologies on stainless steel substrate electrodes were similar to those on Al substrate electrodes.

The influence of current density was exemplified here for the case of a 0.5 M $H_2SO_4$ + 0.5 M $ZnSO_4$ solution. For current densities below 15 mA $cm^{-2}$, the plate surface was not fully covered by the deposit produced during 10 min of deposition. Moreover, local dissolution of the nine sections of the plate revealed that current efficiencies increased with current density up to 45 mA $cm^{-2}$; from 45 to 100 mA $cm^{-2}$, the efficiency remained nearly constant at over 85%, before declining for higher current densities. As shown in Fig. 5, for 30 to 150 mA $cm^{-2}$, the zinc grains were of field-oriented nature, according to the classification suggested by Fischer [23]. The deposit appeared uniform, in spite of the well-identified platelets forming the deposit. For all cases, the orientation of the platelets was consistent with the hexagonal close packed crystal structure of zinc, but their average size increased regularly with current density, from a few μm at 30 mA $cm^{-2}$ to 10–20 μm at 150 mA $cm^{-2}$ (Fig. 5).

### 4.3 Influence of the bath composition

Figure 6 shows the effects of sulfuric acid concentration on current efficiencies for zinc deposition on stainless steel and aluminium, for various zinc(II) concentrations. With stainless steel, low yields were obtained for 0.2 M zinc(II), except for low acid concentrations. As suggested by Alfantazi and Dreisinger [9], the zinc deposit could be corroded in concentrated acidic media, though only for potentials greater than the reversible value. A more likely explanation could be the increase in the exchange current density for hydrogen evolution with increasing sulphuric acid concentration. Increasing the concentration of zinc(II) sulfate to 1.4 M resulted in higher deposition efficiencies, which were little affected by the sulfuric acid concentration in the range 0.1–0.7 M. Higher acid concentrations resulted in decreased zinc deposition yields, contrary to previous

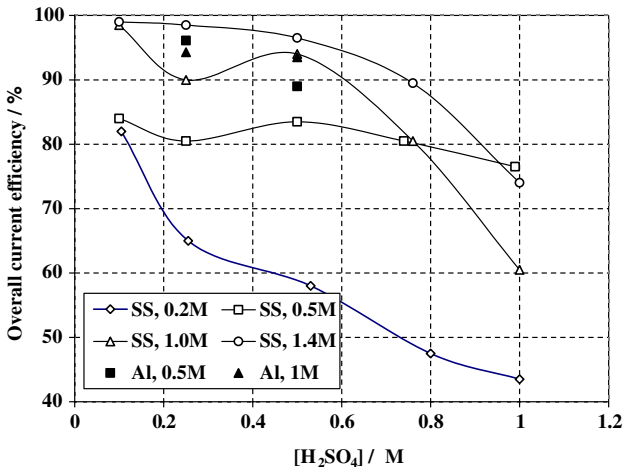


**Fig. 6** Effects of sulfuric acid and zinc sulfate concentrations on the overall current efficiency for zinc deposition on Al or stainless steel in the Hull cell. The uncertainty in the determination was estimated at ±4%

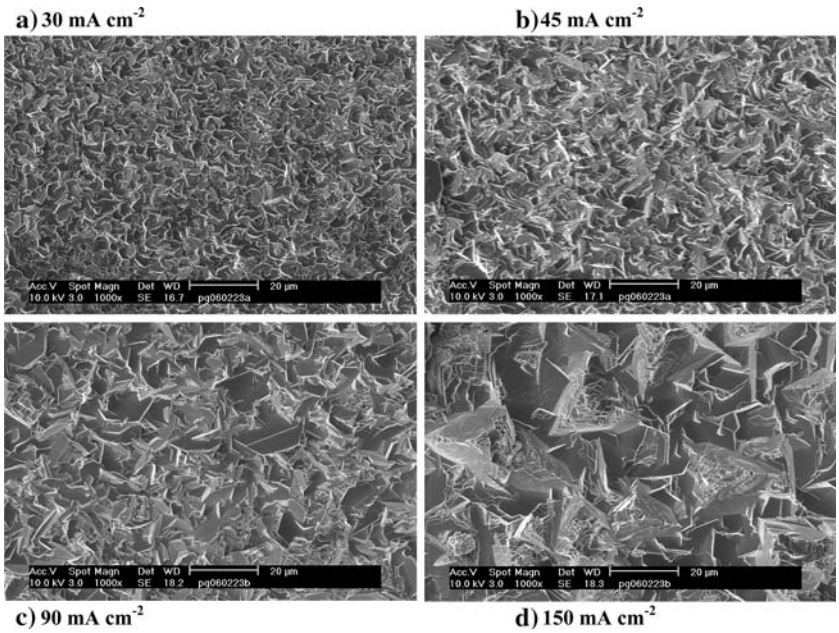


**Fig. 5** Photomicrographs of the zinc deposit produced at various local current densities after 10 min in the Hull cell provided with a stainless steel plate from a 0.5 M $ZnSO_4$, 0.5 M $H_2SO_4$ solution

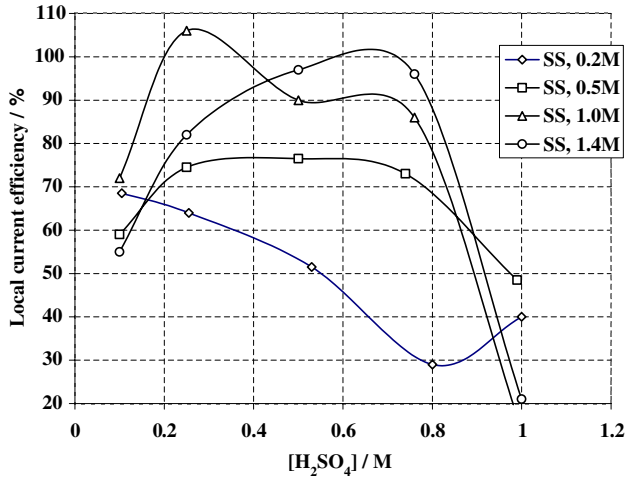


**Fig. 7** Effects of sulfuric acid and zinc sulfate concentrations on current efficiencies for zinc deposition on stainless steel plate in Zone 2 of the Hull cell ($39.4 < j < 51.8$ mA cm$^{-2}$). The uncertainty in the determination was estimated at ±10%

observations reported in [6], but in good agreement with the conclusions of other investigations [7–10]. Reduction of 0.5 or 1 M zinc(II) on a Al plate cathode yielded comparable values of current efficiencies.

Mainly zone 2 was considered in the local analysis, because of its use in defining the optimal current density range, The uncertainty due to the insulating procedure resulted in noticeable dispersion of the results. Nevertheless, current efficiencies at this current density, ca. 45 mA cm$^{-2}$, followed variations with the electrolyte composition (Fig. 7) similar to those of the overall efficiency; lowest values were again obtained with the most dilute zinc(II) solution. In addition, for zinc concentrations of 0.5 M or more, current efficiencies remained nearly constant with the acid concentration below 0.75 M, but decreased drastically in 1 M $H_2SO_4$ media.

Figure 8 shows photomicrographs of the deposits produced at 45 mA cm$^{-2}$ for 10 min, for two levels of zinc(II) and acid concentrations. All deposits were formed of hexagonal platelets described in Sect. 3, but with different sizes and different compactness of the deposit. For a zinc(II) concentration of 0.2 M, finer grains were produced from the 0.25 M sulfuric acid solution (Fig. 8a). The deposit produced from 0.5 M sulfuric acid with 0.2 M zinc(II) sulfate, although regular, did not cover the entire electrode surface, because of significant hydrogen evolution. Use of more concentrated solutions of zinc(II) sulfate, in this case 1 M, resulted in platelets of significant dimensions (near 5 μm), with sharper angles, but forming in a compact deposit, particularly for low acid concentrations: the three-dimensional character of the growth seems to be more pronounced in more acidic baths (Fig. 8d).

## 5 Conclusions

This work aimed to determine suitable conditions of bath composition and current density for optimal deposition of zinc from additive-free zinc sulfate-sulfuric media. Both observations of the deposits produced and analysis of the current yield, showed that deposition has to be carried out from media with zinc(II) concentrations greater than 0.2 M. In agreement with previous investigations, a minimum concentration of zinc(II) sulfate is required to achieve

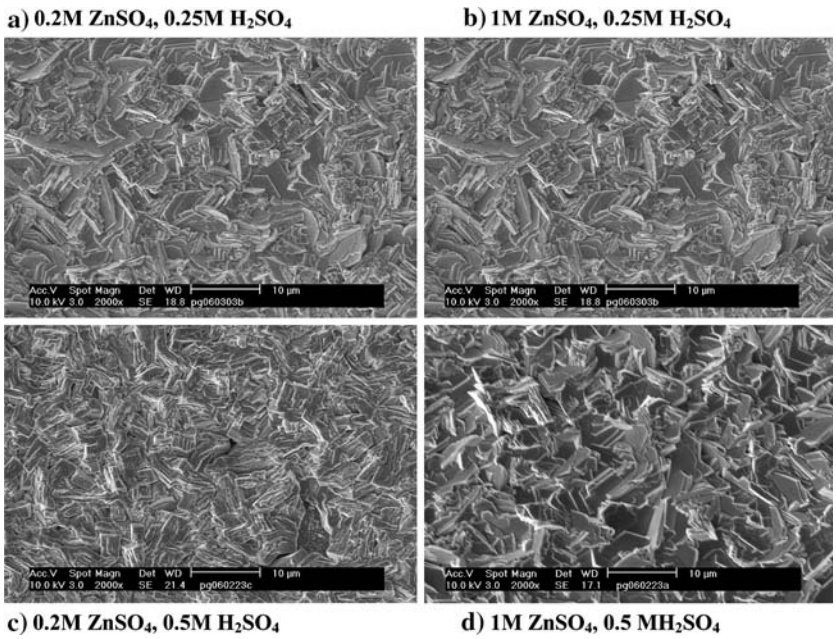


**Fig. 8** Photomicrographs of the zinc deposits on stainless steel plate after 10 min in Zone 2 of the Hull cell ($39.4 < j < 51.8$ mA cm$^{-2}$) with 0.2 or 1 M zinc sulfate and 0.25 or 0.5 M sulfuric acid

efficient deposition. From these results the use is recommended of baths with a $H^+/Zn^{2+}$ concentration ratio ranging from 0.3 to 3, for the production of compact, regular deposits with current efficiencies over 80%.

Such conditions will be used in the envisaged zinc recovery process now being designed for leaching, initially of well-defined zinc oxide dispersed in an inert solid, and later of real oxide wastes, coupled to electrodeposition.

**Acknowledgements** The grant of one author (P.G.) was allocated by Ademe, France. The authors are indebted to Région Lorraine for significant financial support. Thanks are also due to Prof. Geoff Kelsall for a significant contribution to the preparation of the manuscript.

## References

1. Morgan SWK (1985) Zinc and its alloys and compounds. Ellis Horwood, Chichester, UK
2. Monhemius AJ (1980) In: Critical reports in applied chemistry, vol 1. Topics in Non-Ferrous Extractive Metallurgy, Blackwell, Oxford, p 104
3. Sinclair RJ (2005) The extractive metallurgy of zinc. Australasian Institute of Mining and Metallurgy
4. Biegler T, Frazer EJ (1986) J Appl Electrochem 16:654
5. Biegler T, Swift DA (1981) Hydromet 6:299
6. Adcock PA, Ault AR, Newman MG (1985) J Appl Electrochem 15:865
7. Wark W (1979) J Appl Electrochem 9:721
8. Saba AE, Elsherief AE (2000) Hydromet 54:91
9. Alfantazi AM, Dreisinger DB (2001) J Appl Electrochem 31:641
10. McColm TD, Evans JW (2001) J Appl Electrochem 31:411
11. Kelsall GH, Guerra E, Li G, Bestetti (2000) In: Woods R, Doyle FM (eds) International symposium on electrochemistry in mineral and metal processing. Proceedings Volume 2000-14, Electrochemical Society, NJ, p 326
12. Turomshina UF, Stender VV (1955) J Appl Chem USSR 28:151
13. Ault AR, Frazer EJ, Smith GDJ (1988) J Appl Electrochem 18:32
14. Ichino R, Cachet C, Wiart R (1996) Electrochim Acta 41:1031
15. Mackinnon DJ, Brannen JM (1986) J Appl Electrochem 16:127
16. Hosny AY, O'Keefe TJ, James WE (1989) Minerals Eng 2:415
17. Kerby RC, Kraus CJ (1979) In: Cigan JM, Mackey TS, O'Keefe TJ (eds) Lead-Tin-Zinc '80', Proceedings of the World Symposium on Metallurgy and Environmental Control. Metallurgical Society of AIME, Warrendale, p 187
18. Muresan L, Maurin G, Oniciu L, Avram S (1996) Hydromet 40:335
19. Guillaume P, Leclerc N, Lapicque F, Boulanger C, Lecuire JM, accepted in J Hazard Mat
20. Appleby AJ, Chemla M, Kita H, Bronoel G (1982) In: Bard AJ (ed) Encyclopedia on electrochemistry of the elements, vol IX. Marcel Dekker, New York, p 383, Ch. IX-A3
21. Hull RO (1939) Am Electroplat Soc 27:52
22. Norm 50950 DIN (Deutsches Institut für Normung), Mikroscopische Messung der Schichtdicke, TAB 175, (1983) Beuth Verlag GmbH, Berlin
23. Fischer H (1972/1973) Electrodep Surf Treatment 1:239